

## Continuous Orientational Ordering Transition of Carbon Monoxide on Graphite

Y. P. Feng\* and M. H. W. Chan

*Department of Physics, The Pennsylvania State University, University Park, Pennsylvania 16802*

(Received 13 July 1993)

In the compressed incommensurate phase at low temperatures, the molecular axes of CO on graphite are ordered with respect to each other, forming a pinwheel structure. Critical analysis of the heat capacity peak indicates that the transition from the pinwheel to the (orientationally) disordered phase is continuous and belongs to the two-dimensional Ising universality class.

PACS numbers: 64.60.Fr, 64.60.Cn, 68.35.Rh

In last two decades, physisorption systems have provided a rich laboratory for the study of continuous phase transitions in quasi two dimensions. The melting transition of  $^4\text{He}$  on graphite at the  $(\sqrt{3}\times\sqrt{3})R30^\circ$  commensurate coverage is continuous and describable by the three-state Potts model [1]. The melting transitions of monolayer CO on graphite exhibit, depending on the precise coverage, behaviors consistent with the three-state Potts tricritical as well as three-state Potts critical transitions [2]. The order-disorder transition of oxygen on Ru(0001) was found to reside in the four-state Potts universality class [3]. The two-dimensional Ising-like transition has been seen in a number of systems, including the melting of  $^4\text{He}$  on Kr-preplated graphite [4], the liquid-vapor critical transition of submonolayer  $\text{CH}_4$  on graphite [5], the liquid-vapor critical transition of second layer CO on graphite [6], and the layer-critical-point transition of ethylene on graphite [7].

Another important class of phase transitions involves the orientational order of the adsorbed solid layers, in which the molecular axes of nonsymmetrical adsorbates (such as  $\text{C}_2\text{H}_4$ ,  $\text{N}_2$ , and CO) change from being ordered with respect to each other to being randomly oriented. For  $\text{C}_2\text{H}_4$  and  $\text{C}_2\text{D}_4$  on graphite, the ordering transition is found to be broad and diffuse [8]. Although the global monolayer phase diagram of CO on graphite is very similar to that of  $\text{N}_2$  on graphite, the characteristics of the orientational ordering transitions of the two systems, as we shall show below, are distinctively different.

For a commensurate monolayer of  $\text{N}_2$  and CO on graphite at low temperatures ( $T \leq 49$  K), diffraction studies show that the molecules are centered on the sites of a  $(\sqrt{3}\times\sqrt{3})R30^\circ$  structure [9-11]. At even lower temperatures ( $T \leq 28$  K for  $\text{N}_2$  and  $T \leq 26$  K for CO), the molecular axes of both  $\text{N}_2$  and CO are ordered with respect to each other forming the herringbone (HB) structure [see Fig. 1(a)] [9-11]. Whereas the transition from the HB phase into the orientationally disordered (CD) phase exhibits weakly first-order characteristics in the  $\text{N}_2$  case [12], the heat capacity signature related to the same transition for CO is, as we shall show, broad and diffuse. For  $\text{N}_2$ , a small increase in coverage above that of a complete commensurate monolayer causes the HB structure to be compressed uniaxially [13,14]. The transition from this compressed HB phase to the disor-

dered phase also appears to be first order [14]. Instead of uniaxial compression, CO on graphite accommodates the density increase by transforming from a HB phase into a pinwheel (PW) structure where one of every four CO molecules stands normal to the graphite basal plane [see Fig. 1(b)] [10,11,15,16].

The HB and PW structures were first proposed by Harris and Berlinsky as possible phases for  $\text{H}_2$  on graphite [17]. For the HB phase, there are six equivalent ground states: two sublattices each with three possible glide-line orientations. A symmetry analysis showed that such a system can be mapped into the universality class of the two-dimensional Heisenberg model with cubic anisotropy pointing to the six faces of the cube [18,19]. The ordering transition in this model was predicted to be first order [18]. As stated above, this prediction was confirmed experimentally for the HB transition in  $\text{N}_2$  on graphite [12]. In contrast, there are eight equivalent ground states in the PW phase: The pin site of the structure can be at any one of the four sublattices and the rotation of the pinwheel can be either right handed or left handed. This system was shown to belong to the two-dimensional Heisenberg model with cubic anisotropy pointing to the eight corners of the cube [17,19]. The ordering transition for this model was predicted by renormalization group analysis to be continuous with 2D Ising-like critical exponents [19]. We shall present heat

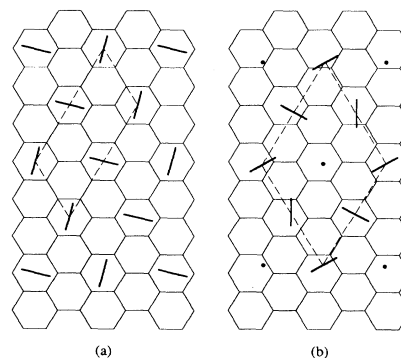


FIG. 1. Schematic diagrams of (a) the orientationally ordered herringbone (HB) structure of CO on graphite, and (b) the orientationally ordered pinwheel (PW) structure of CO on graphite.

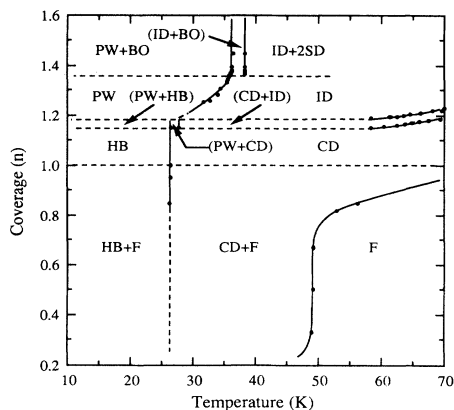


FIG. 2. Proposed phase diagram of CO on graphite. Symbols CD, ID, and F denote, respectively, the commensurate and incommensurate orientationally disordered and fluid phases. BO and 2SD refer to the bilayer orientationally ordered and second layer orientationally disordered solid phases. The phase boundaries shown by solid lines are based on actual heat capacity and vapor isotherm signatures. The dashed lines are deduced by requiring thermodynamic consistency.

capacity results that are consistent with this prediction. It should be noted that the ordering transition of oxygen on Ni(111) studied with low energy electron diffraction (LEED) [20] also appears to reside in this universality class [19].

The experimental arrangement used in this study is similar to earlier works from our laboratory [21]. The substrate is a piece of  $10 \times 10 \times 4$  mm<sup>3</sup> graphite foam having a total surface area of 1.38 m<sup>2</sup>. The thermometer is a Ge-Au film evaporated onto a thin sapphire disk. The temperature resolution is 2 mK for  $T > 25$  K and the resolution in heat capacity value is 0.2%.

In Fig. 2, we show the phase diagram of CO on graphite in the region of interest. A coverage of  $n=1$  is defined as the coverage that separates the commensurate solid-fluid coexistence region from the "pure" commensurate solid phase [2]. Because of the presence of vacancies and promotion of molecules to the second layer, this pure commensurate solid phase is found between  $n=1$  and  $n=1.15$ . The identification of most phases is based on x-ray diffraction [10] and LEED [11] measurements. The boundaries between these phases are based on this heat capacity study. Three heat capacity scans were made at  $n=0.85$ , 0.95, and 1.00 in the commensurate solid phase. For these scans, a weak and broad anomaly centered at about 26 K was found. This anomaly has a FWHM (full width at half maximum) of 2.5 K and a height of only  $0.4k_B$  per molecule. The scan at  $n=0.85$  shown in Fig. 3 is representative of these three scans. This anomaly is identified as related to the disordering "transition" from the HB phase to the orientationally disordered (CD) phase. In comparison, the HB transition in N<sub>2</sub> on graphite at 28 K yields a much sharper heat capacity peak with a height of  $5k_B$  per molecule and a FWHM of 0.5 K

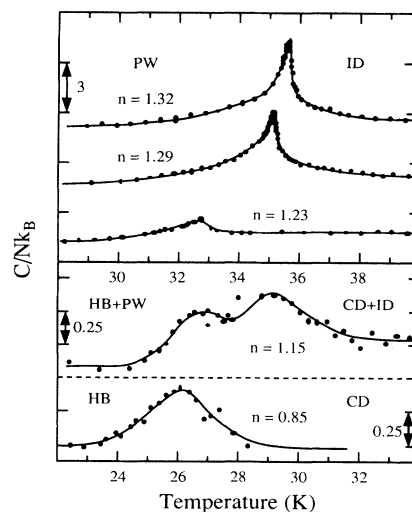


FIG. 3. Heat capacity scans of the orientational ordering transitions at various coverages. The solid lines are guides to the eye only.

(Ref. [12]).

Since the electrostatic quadrupole-quadrupole (EQQ) interaction is primarily responsible for the orientational ordering and the quadrupole moment of CO is 1.5 times stronger than that of N<sub>2</sub> (Ref. [22]), it is surprising that the HB transition in CO is diffuse while in N<sub>2</sub> it is first order. It is also surprising that the transition temperatures in these two systems do not scale with the strength of the EQQ interaction as in the case of the bulk  $\alpha$ - $\beta$  transition [23]. The explanation perhaps lies with the relative magnitude of the adsorbate-substrate interaction represented by a crystal field  $V_c$  and the strength of the EQQ interaction characterized by  $\Gamma$ :  $V_c$  prefers the molecules to lie parallel to the surface of the substrate, whereas  $\Gamma$  prefers a fraction of them to stand normal to the surface [17]. The larger  $\Gamma/V_c$  ratio for CO on graphite may induce frustration in the orientational order, resulting in random tilting of CO molecular axes away from the in-plane direction. Such random tilting was indeed observed in LEED measurement [11] to persist down to at least 15 K and increase with temperature through 26 K where the broad and diffuse heat capacity signal is seen. In this sense, there is no genuine orientational ordering transition for commensurate CO: The broad heat capacity anomaly is probably related to the gradual loss in the in-plane order induced by the tilting of the CO molecular axes. In contrast, there is no evidence of such random tilting in the HB phase of N<sub>2</sub> on graphite at low temperatures [11].

The appearance of the PW phase for CO instead of a uniaxially compressed HB phase at coverages above  $n=1.15$  is also likely a result of CO's larger  $\Gamma/V_c$ . The arrangement in the PW phase with 25% of the CO molecules standing normal to the surface and hence also to other CO molecules clearly takes advantage of the

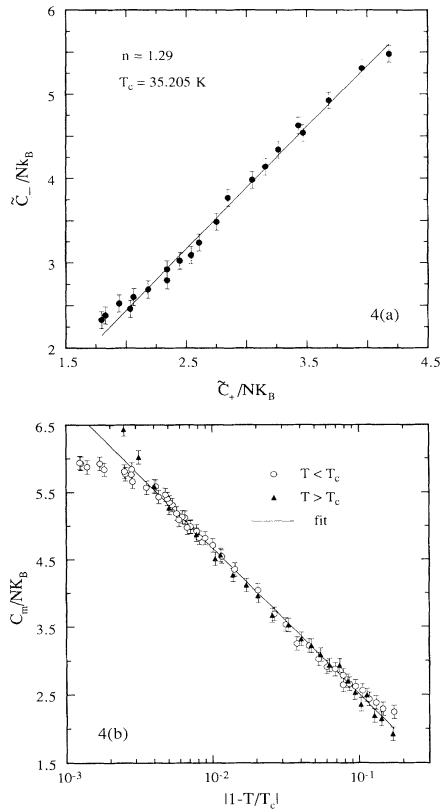


FIG. 4. (a) Correlation between the specific heat below and above the transition temperature at equal reduced temperatures at  $n=1.29$ , confirming the scaling hypothesis. (b) Semilogarithmic plot of the merged specific heat vs the reduced temperature.

stronger EQQ interaction [17]. It should be noted that the weak dipole moment of CO does not appear to play a role in the orientational ordering transitions discussed here. Low temperature heat capacity experiments [24,25] found evidence of dipole-induced end-to-end ordering transition near 5 K, well below the temperature range of the HB and PW transitions.

Nine heat capacity scans at coverages between  $n=1.15$  and  $n=1.36$  were made to study the disordering transition from the PW phase. Four of these scans are shown in Fig. 3. The scan at  $n=1.15$  shows features at 26.5 and 29 K. We interpret this as evidence that this scan traversed within a narrow coexistence region sandwiched between the commensurate and incommensurate phases. These two peaks were related respectively to the transitions from the commensurate HB and the incommensurate PW phases to the orientationally disordered (CD and ID) phases. Upon a slight further increase in coverage ( $n > 1.19$ ), only the PW peak was found. The transition temperature  $T_{PW}$  increased smoothly and the peak sharpened with increasing coverage. At  $n=1.29$ , the peak is  $4k_B$  per molecule in height and 0.5 K in width. The scans

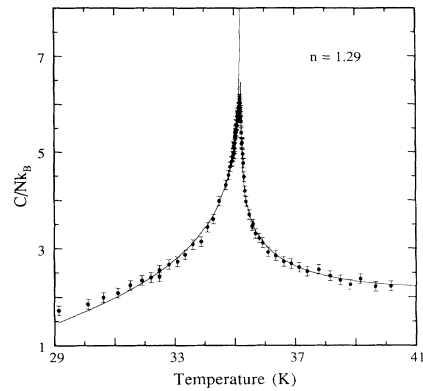


FIG. 5. Experimental (●) and predicted (solid line) values of the specific heat at  $n=1.29$ .

at  $n > 1.36$  show two peaks, relating possibly to the PW transition and the orientational ordering transition of the bilayer that is in coexistence with the incommensurate monolayer [6].

In order to examine the possible critical behavior of the PW transition, we have chosen to analyze the heat capacity peak at  $n=1.29$  which was most carefully taken, following the procedure used by Lederman, Salamon, and Shacklette [26]. Without assuming *a priori* knowledge of the specific heat critical exponent, the specific heat  $C^+$  above and  $C^-$  below the transition temperature  $T_c$  in units of  $k_B$  per molecule are written as

$$C^+ = a^+ (|t|^{-\alpha^+} - 1) / \alpha^+ + b^+ + gt, \tag{1a}$$

$$C^- = a^- (|t|^{-\alpha^-} - 1) / \alpha^- + b^- + gt, \tag{1b}$$

where  $\alpha_+$  and  $\alpha_-$  are the critical exponents above and below  $T_c$ ,  $a^+$ ,  $a^-$ ,  $b^+$ , and  $b^-$ , and  $g$  additional fitting parameters in units of  $k_B$  per molecule, and  $t = (T - T_c) / T_c$  the reduced temperature. The term  $gt$  in Eqs. (1a) and (1b) represents a linear approximation to the specific heat contribution *not* related to the transition. The singular part of the specific heat relating to the ordering transition is then given by

$$\tilde{C}^\pm = C^\pm - gt. \tag{2}$$

By comparing  $\tilde{C}^+$  and  $\tilde{C}^-$  at equal  $|t|$  and applying the scaling hypothesis that  $\alpha_+ = \alpha_- \equiv \alpha$ , we obtain then

$$\tilde{C}^- = (a^- / a^+) \tilde{C}^+ + (b^- - b^+ a^- / a^+), \tag{3a}$$

or equivalently,

$$C^- = (a^- / a^+) C^+ - (1 + a^- / a^+) g |t| + (b^- - b^+ a^- / a^+). \tag{3b}$$

Thus the scaling hypothesis implies that at the same values of  $|t|$ ,  $\tilde{C}^-$  is a linear function of  $\tilde{C}^+$ . To verify this hypothesis, interpolated  $C^-$  data were least squares fitted to a linear function in  $C^+$  in the range of

$0.1 > |t| > 0.004$ . To interpolate  $C^-$  at the desired values of  $|t|$  where  $C^+$  was measured, the experimental values of  $C^-$  were approximated by a high order polynomial in temperature. The coefficients in Eq. (3b) were determined to be  $a^-/a^+ = 1.446$ ,  $g = 3.035$ , and  $(b^- - b^+a^-/a^+) = -0.448$ . The critical temperature  $T_c$  was also taken as a fitting parameter and determined to be 35.205 K, in excellent agreement with the actual data. As shown in Fig. 4(a), the correlation between  $\tilde{C}^-$  and  $\tilde{C}^+$  was indeed verified.

With the parameters determined above,  $\tilde{C}^+$  data were then reflected to equivalent values below  $T_c$  using Eq. (3a). The reflected data and the experimental  $\tilde{C}^-$  are merged as  $C_m$ , which was least squares fitted to the original power law form in Eq. (1b), i.e.,  $C_m = a^- (|t|^{-\alpha} - 1) / \alpha + b^-$ . This fitting procedure, however, results in a vanishingly small critical exponent  $\alpha$ , suggesting a logarithmic dependence in the form of

$$C_m = -a^- \ln|t| + b^- = -2.3a^- \log|t| + b^- . \quad (4)$$

Figure 4(b) confirms such a dependence in the temperature range of  $10^{-1} > |t| > 4 \times 10^{-3}$ . The two parameters of Eq. (4) were determined to be  $a^- = 0.940$  and  $b^- = 0.344$ , respectively. The deviation inside  $|t| = 4 \times 10^{-3}$  is typical of the various continuous phase transitions of monolayer physisorbed on graphite. This deviation is likely to be a consequence of the finite domain sizes on the basal plane of graphite. In Fig. 5, the specific heat calculated using the fitting parameters  $a^+$ ,  $a^-$ ,  $b^+$ ,  $b^-$ ,  $g$ , and  $T_c$  as given above in connection with Eqs. (3b) and (4) is shown in an expanded linear scale together with the actual experimental data. The excellent agreement shown in this figure is consistent with the findings shown in Figs. 4(a) and 4(b).

To conclude, a sharp heat capacity peak is found at the transition from the PW phase to the orientational disordered phase of the compressed incommensurate monolayer of CO on graphite. Critical analysis indicated a logarithmic dependence of  $C$  on  $|t|$  (without an *a priori* assumption of such a dependence), consistent with that expected from a system undergoing a two-dimensional Ising-like transition. The findings of a continuous PW transition for CO (and a weakly first-order HB transition for N<sub>2</sub> on graphite) illustrate, once again, the dominant role of symmetry in determining the nature of phase transitions.

The authors are grateful to S. C. Fain, Jr., for suggesting this experiment and for stimulating discussions. We

also acknowledge useful discussions with W. A. Steele and O. G. Mouritsen, Q. M. Zhang, and H. K. Kim. The work was supported by NSF through Grants No. DMR-8718771 and No. DMR-9022681.

---

\*Present address: Exxon Research and Engineering Company, Annandale, NJ 08801.

- [1] M. Bretz, Phys. Rev. Lett. **38**, 501 (1977); S. Alexander, Phys. Lett. **54A**, 353 (1978).
- [2] Y. P. Feng and M. H. W. Chan, Phys. Rev. Lett. **64**, 2148 (1990).
- [3] P. Piercy and H. Pfnür, Phys. Rev. Lett. **52**, 1124 (1987).
- [4] M. J. Tejwani, O. Ferreira, and O. E. Vilches, Phys. Rev. Lett. **44**, 152 (1980).
- [5] H. K. Kim and M. H. W. Chan, Phys. Rev. Lett. **53**, 170 (1984).
- [6] Y. P. Feng and M. H. W. Chan (to be published).
- [7] Q. M. Zhang *et al.*, Phys. Rev. Lett. **57**, 1456 (1986).
- [8] H. K. Kim *et al.*, Phys. Rev. **B 37**, 3511 (1988).
- [9] R. D. Diehl, M. F. Toney, and S. C. Fain, Jr., Phys. Rev. Lett. **48**, 177 (1982).
- [10] K. Morishige, C. Mowforth, and R. K. Thomas, Surf. Sci. **151**, 289 (1985).
- [11] H. You and S. C. Fain, Jr., Surf. Sci. **151**, 361 (1985).
- [12] A. D. Migone *et al.*, Phys. Rev. Lett. **51**, 192 (1983).
- [13] R. D. Diehl and S. C. Fain, Jr., Surf. Sci. **125**, 116 (1983); Phys. Rev. **B 26**, 4785 (1982).
- [14] Q. M. Zhang, H. K. Kim, and M. H. W. Chan, Phys. Rev. **B 32**, 1820 (1985).
- [15] C. Peters and M. L. Klein, Mol. Phys. **54**, 895 (1985).
- [16] J. Belak, K. Kobashi, and R. D. Eppers, Surf. Sci. **161**, 390 (1985).
- [17] A. B. Harris and A. J. Berlinsky, Can. J. Phys. **57**, 1852 (1979).
- [18] B. Nienhuis, E. K. Riedel, and M. Schick, Phys. Rev. **B 27**, 5625 (1983).
- [19] M. Schick, Surf. Sci. **125**, 94 (1983).
- [20] L. D. Roelofs *et al.*, Phys. Rev. Lett. **46**, 1465 (1981).
- [21] M. H. W. Chan *et al.*, Phys. Rev. **B 30**, 2681 (1984).
- [22] D. E. Stogryn and A. P. Stogryn, Mol. Phys. **11**, 317 (1966).
- [23] W. F. Giauque and J. O. Clayton, J. Am. Chem. **55**, 4875 (1933).
- [24] A. Inaba, T. Shirakami, and H. Chihara, Chem. Phys. Lett. **146**, 63 (1988).
- [25] H. Wiechert and S. A. Arlt, Phys. Rev. Lett. **71**, 2090 (1993).
- [26] F. L. Lederman, M. B. Salamon, and L. W. Shacklette, Phys. Rev. **B 9**, 2981 (1974).